

02 Apr 2007

## Unleaded Drinking Water: Equilibrium Potential Measurements for Monochloramine Disinfectant

Brandi Clark

Follow this and additional works at: <https://scholarsmine.mst.edu/oure>

 Part of the [Inorganic Chemistry Commons](#)

---

### Recommended Citation

Clark, Brandi, "Unleaded Drinking Water: Equilibrium Potential Measurements for Monochloramine Disinfectant" (2007). *Opportunities for Undergraduate Research Experience Program (OURE)*. 194. <https://scholarsmine.mst.edu/oure/194>

This Presentation is brought to you for free and open access by Scholars' Mine. It has been accepted for inclusion in Opportunities for Undergraduate Research Experience Program (OURE) by an authorized administrator of Scholars' Mine. This work is protected by U. S. Copyright Law. Unauthorized use including reproduction for redistribution requires the permission of the copyright holder. For more information, please contact [scholarsmine@mst.edu](mailto:scholarsmine@mst.edu).

***Unleaded Drinking Water:  
Equilibrium Potential Measurements  
for Monochloramine Disinfectant***

***by Brandi Clark***

***Advisor: Dr. Jay Switzer  
Department: Chemistry***

***April 2, 2007***

## Abstract

The strength of monochloramine,  $\text{NH}_2\text{Cl}$ , as an oxidizing agent can be linked to its effect on Pb levels in drinking water. In this study, the equilibrium potential was measured as a function of pH from pH 8 to 12 and compared to a theoretical plot of formal potentials derived from the Nernst equation. The measured equilibrium potential was consistently about 300 mV more negative than the calculated potential –  $\text{NH}_2\text{Cl}$  is a weaker oxidizing agent than predicted. When the measured potentials are plotted on a Pourbaix diagram, it is found that  $\text{NH}_2\text{Cl}$  can oxidize Pb to  $\text{PbO}_2$  only above pH 9.5, while the theoretical values indicate that it can do so at a much lower pH. The validity of the values measured in this experiment is supported by the fact that  $\text{NH}_2\text{Cl}$  has been shown to oxidize Pb to  $\text{Pb}^{2+}$ , not  $\text{PbO}_2$ , at pH 8 (1). The work is important because it is known that  $\text{PbO}_2$  acts as a passivating agent on the inside of lead-bearing plumbing materials.

## Introduction

Due to increasing concerns about chlorinated hydrocarbon byproducts, many drinking water treatment facilities have shifted from free chlorine to monochloramine,  $\text{NH}_2\text{Cl}$ , as a drinking water disinfectant. However, earlier research by the Switzer group has shown that monochloramine oxidizes Pb to soluble  $\text{Pb}^{2+}$  species, while free chlorine passivates Pb by oxidation to  $\text{PbO}_2$  (1). To explain this observation, the group decided that a more in-depth exploration of the electrochemistry of both disinfectants was in order. This study, a measurement of the equilibrium potential for monochloramine, varying the pH between 8 and 12, is part of a larger examination of these electrochemical properties (2). A full paper on this work has been accepted for publication in the ACS journal *Environmental Science & Technology* (manuscript #es062922t). A copy of the paper is attached as Appendix 1.

## Experimental

### *Solution Preparation:*

All  $\text{NH}_2\text{Cl}$  solutions used for these measurements were prepared fresh for each experiment. Solutions were prepared using deionized 18 M $\Omega$ -cm water from a Barnstead NANOpure ultrapure water system. To generate the  $\text{NH}_2\text{Cl}$ , free chlorine was reacted with a five-fold molar excess of aqueous  $\text{NH}_3$ . The source of this free chlorine was a sodium hypochlorite ( $\text{NaOCl}$ ) solution with 10-13 vol% available chlorine. The  $\text{NH}_2\text{Cl}$  concentration was determined via measurement of the absorbance at its characteristic UV absorption maximum – 243 nm ( $\epsilon = 461 \text{ M}^{-1} \text{ cm}^{-1}$ ) to be 0.1 M.

The solutions were buffered using 60 mM NaH<sub>2</sub>PO<sub>4</sub> for pH 7-8, and 60 mM NaHCO<sub>3</sub> or H<sub>3</sub>BO<sub>3</sub> in the pH range of 9 to 12. The pH was then raised to the desired value by slowly adding aqueous NaOH. A Fisher Scientific Accumet Model 15 digital pH meter equipped with an Accumet combination electrode was used to monitor the pH during this process. An Accumet chloride combination ion selective electrode was used to measure the chloride ion concentration – 0.1 M. The working solutions were then deoxygenated by bubbling with argon (99.998 %) for 30 minutes.

#### *Equilibrium Potential Measurement:*

The solution was blanketed with argon while potential measurements were taken relative to the standard calomel electrode (SCE). The equilibrium potential was taken as the open circuit potential after 1000 seconds of measurement. Experiments were performed using a Brinkmann PGSTAT 100 potentiostat controlled by GPES software v. 4.9. An Au electrode was used as the working electrode. The counter electrode was a Pt wire. Although the equilibrium potentials were measured relative to SCE, they are reported versus the normal hydrogen electrode (NHE) by adding 0.242 V to the measured value.

## Results and Discussion

#### *Calculated vs. Measured Equilibrium Potential for Monochloramine:*

The E° values for the reactions of monochloramine in both acidic (pH = 0) and basic (pH = 14) media were calculated by the Switzer Group by summing the free energies of reactions with known equilibrium constants, including the relatively recently proposed equilibrium constant determined by Margerum, *et al.* (3):



This reaction was reversed, to give a  $K_{-1} = 1/K = 2.63 \times 10^{-11}$ , then manipulated using free energies obtained from the known equilibrium constants for the reactions of NH<sub>3</sub> and HOCl under both basic and acidic conditions.

The free energies obtained for these reactions by this summation process can then be converted to standard reduction potentials via the relationship  $\Delta G^\circ = -RT \ln K = -nFE^\circ$ .

This gives the following standard reduction potentials for the NH<sub>2</sub>Cl/Cl<sup>-</sup> couple (2):



Using this result, a plot can be constructed of equilibrium potential as a function of pH (Figure 1), using the Nernst equation:

$$E = E^\circ - RT/nF \ln Q \quad (4)$$

Where  $E$  is the equilibrium potential,  $E^\circ$  is the standard reduction potential,  $R$  is the gas constant ( $8.314 \text{ J mol}^{-1} \text{ K}^{-1}$ ),  $T$  is the absolute temperature,  $n$  is the number of electrons transferred,  $F$  is Faraday's constant ( $96,485 \text{ C}$ ), and  $Q$  is the reaction quotient.

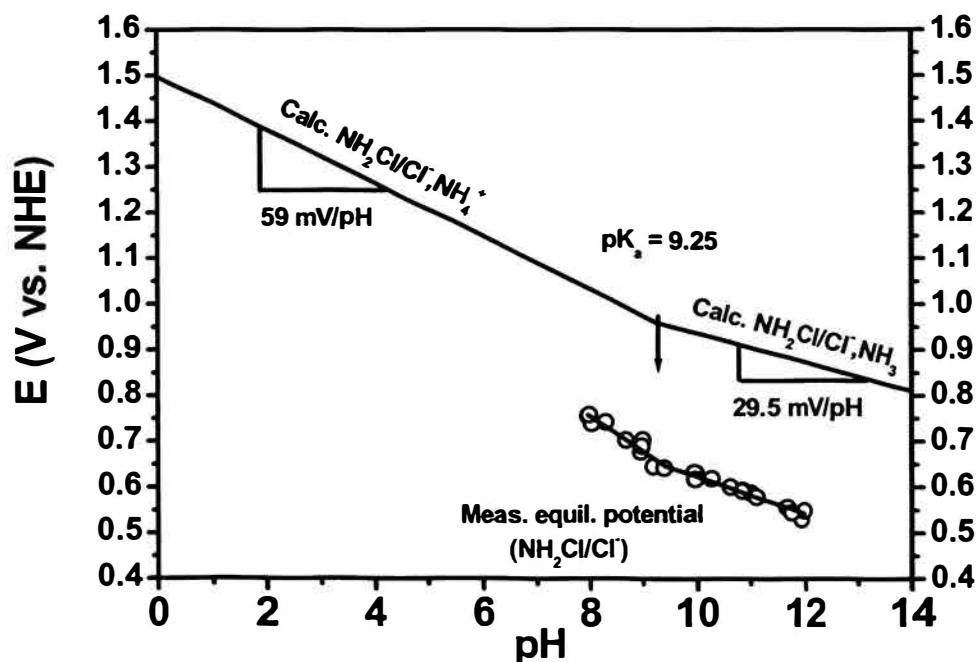


Figure One: Equilibrium Potentials for Monochloramine –  
Measured and Calculated – as a Function of pH

The break in the curve of calculated potentials at  $\text{pH} = 9.25$  is due to the fact that we have reached the  $\text{pK}_a$  of  $\text{NH}_4^+$ , above which it is present as its conjugate base,  $\text{NH}_3$ , and the expression for  $Q$  changes to reflect the basic conditions. That is, the calculated Nernstian slope is  $59 \text{ mV/pH}$  below  $\text{pH} 9.25$  and  $29.5 \text{ mV/pH}$  above  $\text{pH} 9.25$ .

The measured values follow the expected behavior to some extent: The break occurs at a  $\text{pH}$  of  $9.4$  rather than the expected  $9.25$ , and the slope of our measured line is  $75 \text{ mV/pH}$  before the break and  $41 \text{ mV/pH}$  after the break. However, the measured values are about  $300 \text{ mV}$  more

negative than expected, meaning that  $\text{NH}_2\text{Cl}$  is a weaker oxidizing agent than expected theoretically. One explanation is that the proposed equilibrium constant in reaction 1 is incorrect. Another possibility is that the system is more complex than reactions 2 and 3 predict and cannot be explained using these relationships.

#### *Monochloramine as an Oxidizing Agent:*

So, what impact does the 300 mV discrepancy between the calculated and measured potentials have? When the measured equilibrium potentials for monochloramine are plotted on a Pourbaix diagram for the  $\text{Pb}/\text{H}_2\text{O}/\text{CO}_2$  system (Figure 2), constructed by postdoctoral researcher Vishnu Rajasekharan (2), the answer is revealed.

According to the calculated equilibrium potential values,  $\text{NH}_2\text{Cl}$  is a strong enough oxidizing agent to oxidize  $\text{Pb}$  to  $\text{PbO}_2$  at typical drinking water pH values. However, the measured potentials predict that this will only happen above pH 9.5. At lower pH values,  $\text{NH}_2\text{Cl}$  will oxidize  $\text{Pb}$  to only soluble  $\text{Pb}^{2+}$  species. This is confirmed by earlier studies of the effect of  $\text{NH}_2\text{Cl}$  on  $\text{Pb}$  levels done by the group at pH 8, indicating the formation of soluble  $\text{Pb}^{2+}$  species in the presence of  $\text{NH}_2\text{Cl}$  (1).

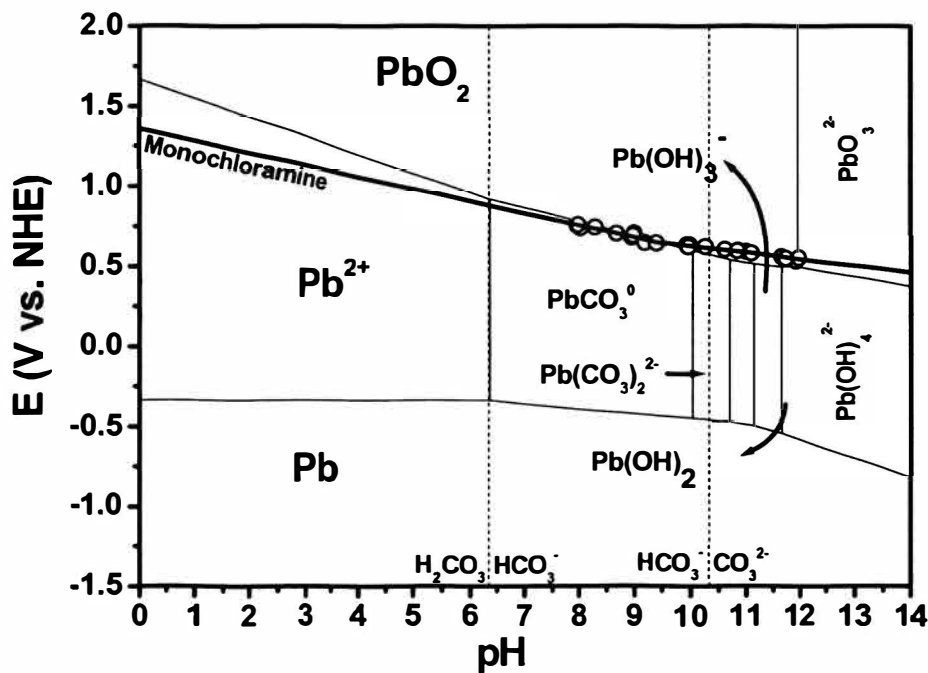


Figure 2: Pourbaix Diagram of  $\text{Pb}/\text{H}_2\text{O}/\text{CO}_2$  System  
With Trendline for Monochloramine Open Circuit Potentials

Therefore, the documented effect of monochloramine on lead levels is supported by the electrochemical evidence obtained in this study, though it is not supported by the theoretical result.

**Acknowledgements:**

Research Advisor, Dr. Jay Switzer. I'm not exaggerating a bit when I say we couldn't have done it without him.

Special thanks to my fellow "water group" members Vishnu and Sansanee for providing patience and papers to read.

In addition to the OURE funding, this work was supported by NSF grants CHE-0437346, and DMR-0504715.

**References:**

- (1) Switzer, J. A.; Rajasekharan, V. V.; Boonsalee, S.; Kulp, E. A.; Bohannon, E. W. Evidence that Monochloramine Disinfectant Could Lead to Elevated Pb Levels in Drinking Water. *Environ. Sci. Technol.* **2006**, *40*, 3384-3387.
- (2) Rajasekharan, V. V.; Clark, B. N.; Boonsalee, S.; Switzer, J. A., "Electrochemistry of free chlorine and monochloramine and its relevance to the presence of Pb in drinking water," *Environ. Sci. Technol.*, manuscript #es062922t, in press. (attached as Appendix I)
- (3) Margerum, D. W.; Schurter, L. M.; Hobson, J.; Moore, E. E. Water chlorination chemistry: nonmetal redox kinetics of chloramine and nitrite ion. *Environ. Sci. Technol.* **1994**, *28*, 331-337.

# Electrochemistry of free chlorine and monochloramine and its relevance to the presence of Pb in drinking water

*Vishnu V. Rajasekharan, Brandi N. Clark, Sansanee Boonsalee, Jay A. Switzer\**

Department of Chemistry and Graduate Center for Materials Research, University of  
Missouri-Rolla, Rolla, MO 65409-1170, USA

\*Corresponding author phone: (573) 341-4383; fax: (573) 341-2071; e-mail:  
jswitzer@umr.edu.

**RECEIVED DATE (to be automatically inserted after your manuscript is accepted  
if required according to the journal that you are submitting your paper to)**

## ABSTRACT

The commonly used disinfectants in drinking water are free chlorine (in the form of HOCl/OCl<sup>-</sup>) and monochloramine (NH<sub>2</sub>Cl). While free chlorine reacts with natural organic matter in water to produce chlorinated hydrocarbon byproducts, there is also concern that NH<sub>2</sub>Cl may react with Pb to produce soluble Pb(II) products – leading to elevated Pb levels in drinking water. In this study, electrochemical methods are used to compare the thermodynamics and kinetics of the reduction of these two disinfectants.



The standard reduction potential for  $\text{NH}_2\text{Cl}/\text{Cl}^-$  was estimated to be +1.45 V in acidic media and +0.74 V in alkaline media versus NHE using thermodynamic cycles. The kinetics of electroreduction of the two disinfectants was studied using an Au rotating disk electrode. The exchange current densities estimated from Koutecky–Levich plots were  $8.2 \times 10^{-5} \text{ A/cm}^2$  and  $4.1 \times 10^{-5} \text{ A/cm}^2$ , and by low overpotential experiments were  $7.5 \pm 0.3 \times 10^{-5} \text{ A/cm}^2$  and  $3.7 \pm 0.4 \times 10^{-5} \text{ A/cm}^2$  for free chlorine and  $\text{NH}_2\text{Cl}$ , respectively. The rate constant for the electrochemical reduction of free chlorine at equilibrium is approximately twice as large as that for the reduction of  $\text{NH}_2\text{Cl}$ . Equilibrium potential measurements show that free chlorine will oxidize Pb to  $\text{PbO}_2$  above pH 1.7, whereas  $\text{NH}_2\text{Cl}$  will oxidize Pb to  $\text{PbO}_2$  only above about pH 9.5, if the total dissolved inorganic carbon (DIC) is 18 ppm. Hence,  $\text{NH}_2\text{Cl}$  is not capable of producing a passivating  $\text{PbO}_2$  layer on Pb, and could lead to elevated levels of dissolved Pb in drinking water.

### **Introduction**

Free chlorine (in the form of hypochlorous acid ( $\text{HOCl}$ ) & hypochlorite anion ( $\text{OCl}^-$ )) and monochloramine ( $\text{NH}_2\text{Cl}$ ) have been used as disinfectants in drinking water (1). They both, however, produce disinfection byproducts. Free chlorine reacts with organic compounds present in water to produce chlorinated hydrocarbons such as trihalomethanes, which are suspected to be carcinogens (2). There is also evidence that  $\text{NH}_2\text{Cl}$  reacts with Pb present in lead service lines, solder, and brass to form soluble  $\text{Pb(II)}$  (3-6). As a consequence, it is important to understand the difference in reactivity of these two disinfectants to ensure the safety of drinking water.

In our earlier work, we showed that  $\text{NH}_2\text{Cl}$  oxidized Pb to soluble  $\text{Pb(II)}$  species, whereas free chlorine produced a passivating layer of  $\text{PbO}_2$  on the Pb (3). Previous

theoretical studies (3,7-10) showed that both  $\text{NH}_2\text{Cl}$  and free chlorine are capable of oxidizing Pb to  $\text{PbO}_2$ , based on the standard reduction potential. However, in real systems only free chlorine forms  $\text{PbO}_2$ , whereas  $\text{NH}_2\text{Cl}$  forms Pb(II) species (3-6,11,12).

The chemical reactivity (9,13-26) and the electroactivity (27-32) of these disinfectants have been studied by other workers. For example, Valentine and co-workers have studied the mechanistic aspects of the reactions between  $\text{NH}_2\text{Cl}$  and Fe(II) in aqueous solutions (15-17). They have presented evidence that the oxidation of Fe(II) to Fe(III) by monochloramine occurs through the formation of a reactive intermediate (amidogen radical ( $\text{NH}_2\dot{\text{N}}$ )) *via* two sequential one-electron steps (15). Wrona and Piela studied the electroreduction of chloramines on rotating Pt and Au electrodes (27). They also suggest that the electroreduction of monochloramine occurs *via* the formation of amidogen radical.

In the present work, we use electrochemical measurements to provide a direct comparison of the kinetics and thermodynamics of the electron transfer reactions of free chlorine and  $\text{NH}_2\text{Cl}$ . The thermodynamics of the reduction of the two disinfectants is compared by calculating the standard reduction potentials from thermodynamic cycles, and by performing equilibrium (i.e., open-circuit) potential measurements. The chemical reversibility and redox activity of the two disinfectants is probed in unstirred solution by cyclic voltammetry. The kinetics of reduction of the two disinfectants is studied using a Au rotating disk electrode (RDE). The RDE is used to control mass transport to the electrode, so that the kinetics can be separated from mass transport by using Koutecky-Levich analysis. Finally, the equilibrium potentials of free chlorine and  $\text{NH}_2\text{Cl}$  are plotted

on a Pourbaix diagram for the Pb-H<sub>2</sub>O-CO<sub>2</sub> system in order to understand the effects of the two disinfectants on the dissolution of Pb.

### **Experimental Section**

All experiments were conducted using deionized 18 M $\Omega$ -cm water from a Barnstead NANOpure ultrapure water system. A sodium hypochlorite (NaOCl) solution with 10-13 vol% available chlorine was used as a source for free chlorine. NH<sub>2</sub>Cl and free chlorine solutions were prepared fresh for each experiment. Free chlorine and NH<sub>2</sub>Cl have characteristic UV absorption bands. The actual concentrations of OCl<sup>-</sup> (at pH 9 the predominant species of free chlorine is OCl<sup>-</sup> (97 %)) and NH<sub>2</sub>Cl were determined spectrophotometrically at 292 nm ( $\epsilon = 350 \text{ M}^{-1}\text{cm}^{-1}$ ) (21) and 243 nm ( $\epsilon = 461 \text{ M}^{-1}\text{cm}^{-1}$ ) (21), respectively. The concentration of NHCl<sub>2</sub> was determined at 206 nm ( $\epsilon = 2100 \text{ M}^{-1}\text{cm}^{-1}$ ) (27).

The NH<sub>2</sub>Cl solutions were prepared by reacting free chlorine with a five-fold molar excess of aqueous NH<sub>3</sub>. The excess NH<sub>3</sub> minimizes the formation of dichloramine (NHCl<sub>2</sub>) (33). To prepare the NH<sub>2</sub>Cl solutions, 5 mL of 100 mM NH<sub>3</sub> was added to a rapidly stirred 20 mL solution of 5 mM NaOCl. The solutions for kinetic studies were buffered at pH 9 with 60 mM NaHCO<sub>3</sub>. The supporting electrolyte was 100 mM Na<sub>2</sub>SO<sub>4</sub>. For the equilibrium potential measurements, 60 mM NaH<sub>2</sub>PO<sub>4</sub> was used as a buffer for pH 7-8, and 60 mM of NaHCO<sub>3</sub> or H<sub>3</sub>BO<sub>3</sub> were used as buffers in the pH range of 9 to 12. It is important to note that these buffers can be used to study the electrochemistry of NH<sub>2</sub>Cl and free chlorine on inert electrodes such as Au or Pt, but they would complicate studies involving Pb or PbO<sub>2</sub> electrodes because of the formation of insoluble Pb(II) carbonates and phosphates.

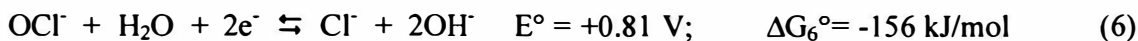
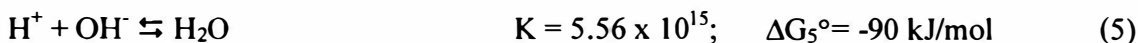
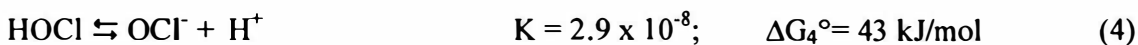
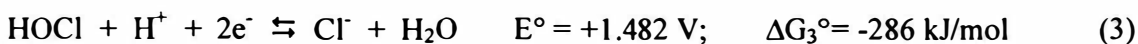
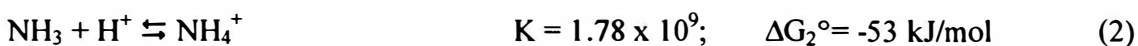
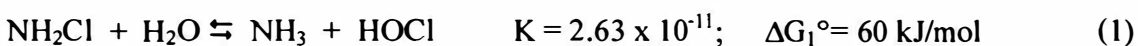
A Fisher Scientific Accumet Model 15 digital pH meter equipped with an Accumet combination electrode was used for the pH measurements. An Accumet chloride combination ion selective electrode was used to measure the chloride ion concentration. A Hach ammonia gas sensing combination electrode was used to measure the total excess ammonia present in the  $\text{NH}_2\text{Cl}$  containing solutions. Typically, approximately 4 mM total ammonia was present after the formation of  $\text{NH}_2\text{Cl}$ .

Electrochemical experiments were performed using a Brinkmann PGSTAT 100 potentiostat controlled by GPES software v. 4.9. The experiments were run at room temperature in a cell that was not thermostatted. A polycrystalline Au electrode (Pine instruments, USA) of geometric area  $0.196 \text{ cm}^2$  was used for stationary and rotating disk studies. A MSR speed controller from Pine instrument company was used to vary the rotation rates. The counter electrode was a Pt wire. A saturated calomel electrode (SCE) was used as the reference electrode in all electrochemical experiments. All potentials, except equilibrium potentials, are reported versus the SCE. The equilibrium potentials are reported versus the normal hydrogen electrode (NHE) by adding 0.242 V to the potential measured versus SCE. The equilibrium potentials were measured on an Au electrode after equilibrating for 1000 s. Equilibrium potentials must be measured with a high impedance voltmeter or electrometer, so that the equilibrium is not shifted by current flow. In our studies the Brinkmann PGSTAT 100 potentiostat (input impedance greater than 100 Gohm) was used for these measurements. The working solutions were deoxygenated by bubbling with argon (99.998 %)(BOC gases).

## **Results and Discussion**

### Calculation of the standard reduction potential of $\text{NH}_2\text{Cl}$

The standard reduction potential of the  $\text{NH}_2\text{Cl}/\text{Cl}^-$  couple in both acidic and alkaline solutions can be estimated using the following parameters: the equilibrium constants for Equation 1 (20), 2, 4 & 5 and the standard reduction potentials for  $\text{HOCl}/\text{Cl}^-$  and  $\text{OCl}^-/\text{Cl}^-$ , (Equations 3 & 6) (34). The relationship between the free energy, equilibrium constant and standard reduction potential ( $\Delta G^\circ = -RT \ln K = -nFE^\circ$ ) was then used to calculate the  $\Delta G^\circ$  for the reactions below. By convention, the equilibrium constants are shown without units, although they are based on molar concentrations.



The standard reduction potentials of  $\text{NH}_2\text{Cl}$  in acidic and alkaline solutions can be determined by standard thermodynamic cycles. To estimate  $\Delta G_a^\circ$  for the reduction reaction of  $\text{NH}_2\text{Cl}$  in acidic media (i.e.,  $\text{pH} = 0$ ), the  $\Delta G^\circ$ s for the elementary reactions shown in Equations 1, 2 & 3 are summed, as shown in Equation 7.

$$\Delta G_a^\circ = \Delta G_1^\circ + \Delta G_2^\circ + \Delta G_3^\circ = -279 \text{ kJ/mol} \quad (7)$$

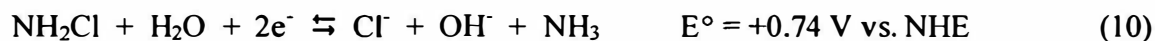
From Equation 7 the standard reduction potential for  $\text{NH}_2\text{Cl}$  can be determined, and is given below in Equation 8



To estimate  $\Delta G_b^\circ$  for the reduction reaction of  $\text{NH}_2\text{Cl}$  in alkaline media (i.e.,  $\text{pH} = 14$ ), the  $\Delta G^\circ$ s for the elementary reactions shown in Equations 1, 4, 5 & 6 are summed, as shown in Equation 9.

$$\Delta G_b^\circ = \Delta G_1^\circ + \Delta G_4^\circ + \Delta G_5^\circ + \Delta G_6^\circ = -143 \text{ kJ/mol} \quad (9)$$

From Equation 9 the standard reduction potential for  $\text{NH}_2\text{Cl}$  can be determined, and is given below in Equation 10



#### Equilibrium potentials for $\text{NH}_2\text{Cl}$

Equilibrium (i.e., open-circuit) potential measurements for  $\text{NH}_2\text{Cl}$  were performed on a Au electrode in solutions containing equimolar quantities of the redox species in 60 mM buffered solutions. Equilibrium potentials are also referred to in the literature as oxidation-reduction potentials (ORPs). James *et al.* have previously used ORP measurements to compare the relative impact of various disinfectants on metallic plumbing material solubility and speciation (35). Figure 1 shows a plot of the measured (open circles) equilibrium potentials for  $\text{NH}_2\text{Cl}$  as a function of pH. Figure 1 also compares the measured equilibrium potentials to calculated formal potentials. The standard reduction potentials for Equations 8 & 10 are for all of the reactants and products at unit activity. Formal potentials for these reactions at other concentrations and pHs can be calculated from the Nernst equation (Equation 11).

$$E = E^\circ - \frac{RT}{nF} \ln Q \quad (11)$$

where  $E$  is the formal potential (V),  $E^\circ$  is the standard reduction potential (V),  $R$  is the molar gas constant ( $8.314 \text{ J mol}^{-1} \text{ K}^{-1}$ ),  $T$  is the absolute temperature (K),  $n$  is the number

of electrons transferred,  $F$  is Faraday's constant (96,485 C), and  $Q$  is the reaction quotient (dimensionless).

The formal reduction potentials (solid lines) calculated from Equation 11 are shown in Figure 1. The formal potentials were calculated from Equation 11 with  $[\text{NH}_2\text{Cl}] = [\text{Cl}^-] = 1 \text{ mM}$ , and  $[\text{NH}_3] + [\text{NH}_4^+] = 4 \text{ mM}$ . For the calculated formal potentials, a Nernstian slope of 59 mV/pH is predicted at low pH, and a slope of 29.5 mV/pH is predicted at high pH. The change in slope at pH 9.25 is due to the fact that  $\text{NH}_4^+$  ( $\text{pK}_a = 9.25$ ) is formed below the  $\text{pK}_a$ , and  $\text{NH}_3$  is formed above the  $\text{pK}_a$ . The slope of a linear fit for the values of measured equilibrium potentials is 75 mV/pH below pH 9.4 and 41 mV/pH above pH 9.4.

The measured equilibrium potential is approximately 300 mV more negative than the calculated formal potential at pH 9.25. This suggests that there is either an error in the calculated standard reduction potentials for Equations 8 and 10 due to an error in the equilibrium constant for Equation 1 (9,36), or that the reduction of  $\text{NH}_2\text{Cl}$  does not proceed by the reactions shown in Equations 8 and 10. One explanation is that there are competing reactions involving reactive amidogen ( $\text{NH}_2^\bullet$ ) radical intermediates. The radicals could either couple to produce hydrazine or react with bicarbonate in solution. In either case, the measured equilibrium potential would be different from the calculated formal potential. Valentine and co-workers have shown evidence for the formation of the amidogen radical during oxidation of Fe(II) (15). They have also proposed that these radicals can be scavenged by bicarbonate or that radical-radical coupling can occur to produce hydrazine. Piela and Wrona have also suggested that the amidogen radical is

produced in the rate determining, one-electron step during the electroreduction of  $\text{NH}_2\text{Cl}$  (27).

#### Cyclic voltammetry of $\text{OCl}^-$ and $\text{NH}_2\text{Cl}$

Figures 2a and b show cyclic voltammograms (CVs) of (a)  $\text{OCl}^-$  and (b)  $\text{NH}_2\text{Cl}$  in Ar-purged solutions containing 60 mM  $\text{NaHCO}_3$  and 0.1 M  $\text{Na}_2\text{SO}_4$  at pH 9 for various concentrations of the two disinfectants. The CVs were run in an unstirred solution at a scan rate of 50 mV/s on a Au stationary electrode. In the CVs,  $\text{OCl}^-$  and  $\text{NH}_2\text{Cl}$  both show single cathodic peaks at approximately 0.32 V and 0.03 V, respectively. There are no significant anodic peaks corresponding to these cathodic peaks, showing that the reactions are electrochemically irreversible reductions. In oxygen-saturated solutions (not shown), both solutions show an additional cathodic peak at -0.25 V due to the reduction of dissolved oxygen. The cathodic peak currents for the reduction of both  $\text{OCl}^-$  and  $\text{NH}_2\text{Cl}$  increase linearly as the concentrations of the two disinfectants are increased.

#### Rotating disk studies of the reduction of $\text{OCl}^-$ and $\text{NH}_2\text{Cl}$

The standard heterogeneous rate constant ( $k_0$ ) for the reduction of  $\text{OCl}^-$  and  $\text{NH}_2\text{Cl}$  can be determined at the equilibrium potential (i.e., zero driving force) using the rotating disk electrode by both Koutecky–Levich analysis, and by using a linear approximation to the Butler-Volmer equation at very low overpotential (37). Figures 3a and b show linear sweep voltammograms of 1.7 mM  $\text{OCl}^-$  and  $\text{NH}_2\text{Cl}$ , respectively, in an Ar-purged solution containing 60 mM  $\text{NaHCO}_3$  and 0.1 M  $\text{Na}_2\text{SO}_4$  at pH 9 at a scan rate of 50 mV/s on a Au rotating disk electrode at various rotation rates. Both disinfectants show mixed kinetic-diffusion regimes at intermediate potentials and mass-transport-



limited currents at high overpotentials. Koutecky-Levich analysis was done in the mixed kinetic-diffusion regimes. The Koutecky–Levich equation is shown in Equation 12.

$$1/i = 1/i_k + 1/i_l = 1/i_k + 1/(0.62nFAD^{2/3}\omega^{1/2}\nu^{-1/6}C) \quad (12)$$

where  $i$  is the measured current (A),  $i_k$  is the current in the absence of any mass-transport effects (A),  $i_l$  is the limiting current at high overpotential (A),  $n$  is the number of electrons transferred,  $F$  is Faraday's constant (96,485 C),  $A$  is the electrode area ( $\text{cm}^2$ ),  $D$  is the diffusion coefficient ( $\text{cm}^2\text{s}^{-1}$ ),  $\omega$  is the angular frequency of rotation ( $\text{s}^{-1}$ ),  $\nu$  is the kinematic viscosity ( $\text{cm}^2\text{s}^{-1}$ ) and  $C$  is the concentration ( $\text{mol}/\text{cm}^3$ ).

Figure 4 shows Koutecky–Levich plots of  $1/i$  versus  $1/\omega^{1/2}$  for (a)  $\text{OCl}^-$  and (b)  $\text{NH}_2\text{Cl}$  at a series of overpotentials ( $\eta$ ). The overpotentials were approximated by taking the difference between the applied electrode potential and the open circuit potentials of 0.67 V for  $\text{OCl}^-$  and 0.47 V for  $\text{NH}_2\text{Cl}$ . Straight lines are observed for both disinfectants with intercepts corresponding to their kinetic currents ( $i_k$ ) for a wide range of overpotentials (0.375 to 0.575 V). The kinetic currents ( $i_k$ ) can be converted to rate constants ( $k_f$ ) using equation 13.

$$i_k = nFAk_fC \quad (13)$$

where  $n$  is the number of electrons transferred,  $F$  is Faraday's constant (C),  $A$  is the electrode area ( $\text{cm}^2$ ),  $k_f$  is the forward rate constant ( $\text{cm}/\text{s}$ ), and  $C$  is the concentration ( $\text{mol}/\text{cm}^3$ ). We assumed  $n = 2$  for these calculations.

Figure 5 shows a plot of  $\ln k_f(E)$  versus overpotential ( $\eta$ ). This plot should have a slope of  $-\alpha F/RT$  and an intercept equal to  $\ln(k^0)$  (37). The  $\alpha$  value determined from the slope for  $\text{OCl}^-$  was 0.3, and for  $\text{NH}_2\text{Cl}$  was 0.2. The  $k^0$  value obtained for  $\text{OCl}^-$  was  $2.5 \times 10^{-4}$  cm/s and, for  $\text{NH}_2\text{Cl}$  was  $1.2 \times 10^{-4}$  cm/s. The exchange current densities ( $j_0$ )

determined from these  $k^{\circ}$  values using Equation 13 and normalizing for the electrode area were  $8.2 \times 10^{-5} \text{ A/cm}^2$  and  $4.1 \times 10^{-5} \text{ A/cm}^2$  for  $\text{OCl}^-$  and  $\text{NH}_2\text{Cl}$ , respectively. These values show that at equilibrium, the rate constant for the reduction of  $\text{OCl}^-$  is approximately twice that of  $\text{NH}_2\text{Cl}$ .

The standard heterogeneous rate constant  $k_0$  can also be estimated from linear sweep voltammograms at low overpotential, where mass-transport effects are minimal. For small values of overpotential,  $\eta$ , the Butler–Volmer equation is approximated by Equation 14 (37,38).

$$j = -j_0 F \eta / (RT) \quad (14)$$

where  $j$  is the measured current density ( $\text{A/cm}^2$ ),  $j_0$  is the exchange current density ( $\text{A/cm}^2$ ),  $F$  is Faraday's constant (C),  $\eta$  is the applied overpotential (V),  $R$  is the molar gas constant ( $\text{Jmol}^{-1}\text{K}^{-1}$ ), and  $T$  is the absolute temperature ( $F/RT = 38.92 \text{ V}^{-1}$  at 298 K). Figure 6 shows plots of  $j$  versus  $\eta$  for 1.7 mM  $\text{OCl}^-$  and  $\text{NH}_2\text{Cl}$  in an Ar-purged solution containing 60 mM  $\text{NaHCO}_3$  and 0.1 M  $\text{Na}_2\text{SO}_4$  at pH 9. The voltammograms were run at a scan rate of 1 mV/s on a Au electrode at 900 rpm. The slopes of the  $j$  versus  $\eta$  plots for the disinfectants were not dependent on the rotation rate. The slopes of five different rotation rates (700 rpm, 900, 1100, 1300, and 1500) were obtained to estimate the error involved in the measurements. The exchange current densities,  $j_0$ , determined from these slopes are  $7.5 \pm 0.3 \times 10^{-5} \text{ A/cm}^2$  for  $\text{OCl}^-$  and  $3.7 \pm 0.4 \times 10^{-5} \text{ A/cm}^2$  for  $\text{NH}_2\text{Cl}$ . The  $k^{\circ}$  values determined from the  $j_0$  values are  $2.3 \pm 0.1 \times 10^{-4}$  and  $1.1 \pm 0.1 \times 10^{-4} \text{ cm/s}$  for  $\text{OCl}^-$  and  $\text{NH}_2\text{Cl}$ , respectively.

The exchange current densities and standard heterogeneous rate constant for  $\text{OCl}^-$  and  $\text{NH}_2\text{Cl}$  are summarized in Table 1 for measurement by both Koutecky–Levich

analysis and by the linear approximation of the Butler-Volmer equation at low overpotential. Both methods show that at equilibrium (zero driving force), the rate constant for the reduction of  $\text{OCl}^-$  is approximately twice that of  $\text{NH}_2\text{Cl}$ .

#### Measured equilibrium potential as a diagnostic tool to determine the stability of Pb

Figure 7 shows the Pourbaix diagram for the Pb-H<sub>2</sub>O-CO<sub>2</sub> system along with the measured formal potentials of  $\text{NH}_2\text{Cl}$  and free chlorine. This diagram is constructed to determine the stability of Pb in the presence of these disinfectants. Figure 7 is similar to the one constructed by Schock and co-workers (39-41). The concentration of the dissolved Pb(II) species in Figure 7 is fixed at the action level of Pb in drinking water ( $7.2 \times 10^{-8}$  M) (15 ppb). The concentration of total dissolved inorganic carbon (DIC) is chosen as 1.5 mM (18 ppm), which is the value previously used by Schock *et al.* (40). The Gibbs free energies of formation of the different Pb species at 298 K and 1 atm are used to calculate the equilibrium constants and standard reduction potentials for the chemical and electrochemical reactions of different Pb species (41). The lead carbonate species are included in Figure 7, due to the importance of carbonate compounds of the Pb(II) species (41-44). In our previous study we observed a lead carbonate phase (hydrocerrusite ( $\text{Pb}_3(\text{CO}_3)_2(\text{OH})_2$ )), when a Pb film was exposed to a solution containing  $\text{NH}_2\text{Cl}$  (3).

In Figure 7, the measured equilibrium potentials for  $\text{NH}_2\text{Cl}/\text{Cl}^-$  are more negative than those of the free chlorine species for pH values that are relevant to drinking water. This is a direct indication that  $\text{NH}_2\text{Cl}$  is a thermodynamically weaker oxidizing agent than free chlorine. Figure 7 shows that free chlorine is thermodynamically capable of oxidizing Pb to  $\text{PbO}_2$  above pH 1.7, whereas  $\text{NH}_2\text{Cl}$  is thermodynamically capable of

oxidizing Pb to PbO<sub>2</sub> only above about pH 9.5 at the DIC level of 18 ppm. Even above pH 9.5, the driving force for the production of PbO<sub>2</sub> by NH<sub>2</sub>Cl is small. It is also dependent on the concentration of Pb(II) used to calculate the Pourbaix diagram, and on the concentration of dissolved inorganic carbon. The relationship of the measured equilibrium potentials with the Pb(II)/PbO<sub>2</sub> boundary in the Pourbaix diagram is consistent with our previous *in-situ* Pb dissolution studies at pH 8, in which NH<sub>2</sub>Cl oxidizes Pb to Pb(II) species such as Pb<sub>3</sub>(CO<sub>3</sub>)<sub>2</sub>(OH)<sub>2</sub>, whereas free chlorine oxidizes Pb to insoluble, tetravalent PbO<sub>2</sub> (3). The measurement of equilibrium potentials in drinking water may prove to be a useful diagnostic tool to determine the stability of Pb in the presence of these disinfectants.

ACKNOWLEDGMENT: This work was supported by NSF grants CHE-0437346, and DMR-0504715.

**References**

- (1) White, G. C. *Handbook of Chlorination and Alternative Disinfectants*; 2nd ed.; Van Nostrand Reinhold Company: New York, 1986.
- (2) U. S. Environmental Protection Agency. National interim primary drinking water regulations; control of trihalomethanes in drinking water. *Fed. Regist.* **1979**, *44*, 68624-68707.
- (3) Switzer, J. A.; Rajasekharan, V. V.; Boonsalee, S.; Kulp, E. A.; Bohannon, E. W. Evidence that Monochloramine Disinfectant Could Lead to Elevated Pb Levels in Drinking Water. *Environ. Sci. Technol.* **2006**, *40*, 3384-3387.
- (4) Edwards, M.; Dudi, A. Role of chlorine and chloramine in corrosion of lead-bearing plumbing materials. *J. Am. Water Works Assoc.* **2004**, *96*, 69-81.
- (5) Renner, R. Plumbing the depths of D.C.'s drinking water crisis. *Environ. Sci. Technol.* **2004**, *38*, 224A-227A.
- (6) Renner, R. Chloramines again linked to lead in drinking water. *Environ. Sci. Technol.* **2005**, *39*, 314A.
- (7) Jolly, W. L. The thermodynamic properties of chloramine, dichloramine, and nitrogen trichloride. *J. Phys. Chem.* **1956**, *60*, 507-508.
- (8) Soulard, M.; Bloc, F.; Hatterer, A. Diagrams of existence of chloroamines and bromoamines in aqueous solution. *J. Chem. Soc., Dalton Trans.* **1981**, 2300-2310.
- (9) Gray, E. T., Jr.; Margerum, D. W.; Huffman, R. P. Chloramine equilibria and the kinetics of disproportionation in aqueous solution. *ACS Symp. Ser.* **1978**, *82*, 264-277.
- (10) Wrona, P. K. Electrode processes of chloramines in aqueous solutions. *Journal of Electroanalytical Chemistry* **1998**, *453*, 197-204.
- (11) Renner, R. More chloramine complications. *Environ. Sci. Technol.* **2004**, *38*, 342A-343A.
- (12) Renner, R. Chloramine's effect on lead in drinking water. *Environ. Sci. Technol.* **2006**, *40*, 3129-3130.
- (13) Yiin, B. S.; Margerum, D. W. Non-metal redox kinetics: reactions of trichloramine with ammonia and with dichloramine. *Inorg. Chem.* **1990**, *29*, 2135-2141.
- (14) Yiin, B. S.; Walker, D. M.; Margerum, D. W. Nonmetal redox kinetics: general-acid-assisted reactions of chloramine with sulfite and hydrogen sulfite. *Inorg. Chem.* **1987**, *26*, 3435-3441.
- (15) Vikesland, P. J.; Valentine, R. L. Reaction Pathways Involved in the Reduction of Monochloramine by Ferrous Iron. *Environ. Sci. Technol.* **2000**, *34*, 83-90.
- (16) Vikesland, P. J.; Valentine, R. L. Iron Oxide Surface-Catalyzed Oxidation of Ferrous Iron by Monochloramine: Implications of Oxide Type and Carbonate on Reactivity. *Environ. Sci. Technol.* **2002**, *36*, 512-519.
- (17) Vikesland, P. J.; Valentine, R. L. Modeling the kinetics of ferrous iron oxidation by monochloramine. *Environ. Sci. Technol.* **2002**, *36*, 662-668.
- (18) Snyder, M. P.; Margerum, D. W. Kinetics of chlorine transfer from chloramine to amines, amino acids, and peptides. *Inorg. Chem.* **1982**, *21*, 2545-2550.
- (19) Margerum, D. W.; Gray, E. T., Jr.; Huffman, R. P. Chlorination and the formation of N-chloro compounds in water treatment. *ACS Symp. Ser.* **1978**, *82*, 278-291.

- (20) Margerum, D. W.; Schurter, L. M.; Hobson, J.; Moore, E. E. Water chlorination chemistry: nonmetal redox kinetics of chloramine and nitrite ion. *Environ. Sci. Technol.* **1994**, *28*, 331-337.
- (21) Kumar, K.; Day, R. A.; Margerum, D. W. Atom-transfer redox kinetics: general-acid-assisted oxidation of iodide by chloramines and hypochlorite. *Inorg. Chem.* **1986**, *25*, 4344-4350.
- (22) Kumar, K.; Margerum, D. W. Kinetics and mechanism of general-acid-assisted oxidation of bromide by hypochlorite and hypochlorous acid. *Inorg. Chem.* **1987**, *26*, 2706-2711.
- (23) Gerritsen, C. M.; Margerum, D. W. Non-metal redox kinetics: hypochlorite and hypochlorous acid reactions with cyanide. *Inorg. Chem.* **1990**, *29*, 2757-2762.
- (24) Fogelman, K. D.; Walker, D. M.; Margerum, D. W. Nonmetal redox kinetics: hypochlorite and hypochlorous acid reactions with sulfite. *Inorg. Chem.* **1989**, *28*, 986-993.
- (25) Dodd, M. C.; Vu, N. D.; Ammann, A.; Le, V. C.; Kissner, R.; Pham, H. V.; Cao, T. H.; Berg, M.; von Gunten, U. Kinetics and Mechanistic Aspects of As(III) Oxidation by Aqueous Chlorine, Chloramines, and Ozone: Relevance to Drinking Water Treatment. *Environ. Sci. Technol.* **2006**, *40*, 3285-3292.
- (26) Conocchioli, T. J.; Hamilton, E. J., Jr.; Sutin, N. Formation of iron(IV) in the oxidation of iron(II). *J. Am. Chem. Soc.* **1965**, *87*, 926-927.
- (27) Piela, B.; Wrona, P. K. Electrochemical Behavior of Chloramines on the Rotating Platinum and Gold Electrodes. *J. Electrochem. Soc.* **2003**, *150*, E255-E265.
- (28) Shin-ya Kishioka, T. K., Akifumi Yamada,. Electrochemical Determination of a Free Chlorine Residual Using Cathodic Potential-Step Chronocoulometry. *Electroanalysis* **2005**, *17*, 724-726.
- (29) Marks, H. C.; Bannister, G. L.; Glass, J. R.; Herrigel, E. Amperometric methods in the control of water chlorination. *Anal. Chem.* **1947**, *19*, 200-204.
- (30) Jenkins, E. N. Reactions of hypochlorous acid and sodium hypochlorite at the dropping-mercury electrode. *J. Chem. Soc.* **1951**, 2627-2630.
- (31) Heller, K.; Jenkins, E. N. Behavior of hypochlorite and of N-chloroamines at the dropping-mercury electrode. *Nature (London, United Kingdom)* **1946**, *158*, 706.
- (32) Evans, O. M. Voltammetric determination of the decomposition rates of combined chlorine in aqueous solution. *Anal. Chem.* **1982**, *54*, 1579-1582.
- (33) Brodtmann, N. V., Jr.; Russo, P. J. The use of chloramine for reduction of trihalomethanes and disinfection of drinking water. *J. Am. Water Works Assoc.* **1979**, *71*, 40-42.
- (34) Lide, D. R., Ed. *CRC Handbook of Chemistry and Physics*; 86th ed.; Taylor & Francis Group: New York, 2005-2006.
- (35) James, C. N.; Copeland, R. C.; Lytle, D. A. Relationships between oxidation-reduction potential, oxidant, and pH in drinking water. *Proc. AWWA Water Quality Technology Conference*, San Antonio, Texas, November 14-18, 2004; pp 1-13.
- (36) Anbar, M.; Yagil, G. The hydrolysis of chloramine in alkaline solution. *J. Am. Chem. Soc.* **1962**, *84*, 1790-1796.
- (37) Bard, A. J.; Faulkner, L. R. *Electrochemical Methods: Fundamentals and Applications*; 2nd ed.; John Wiley & Sons: New York, 2001.

- (38) Switzer, J. A.; Kothari, H. M.; Bohannon, E. W. Thermodynamic to Kinetic Transition in Epitaxial Electrodeposition. *J. Phys. Chem. B* **2002**, *106*, 4027-4031.
- (39) Lytle, D. A.; Schock, M. R. The formation of Pb(IV) oxides in chlorinated water. *J. Am. Water Works Assoc.* **2005**, *97*, 102-114.
- (40) Schock, M. R.; Harmon, S. M.; Swertfeger, J.; Lohmann, R. Tetravalent lead: a hitherto unrecognized control of tap water lead contamination. *Proceedings - Water Quality Technology Conference* **2001**, 2270-2291.
- (41) Schock, M. R.; Wagner, I.; Oliphant, R. J. In *Internal Corrosion of Water Distribution Systems*; 2 ed.; AWWA, Ed.; AWWA: Denver, 1996; pp 131-230.
- (42) Schock, M. R. Response of lead solubility to dissolved carbonate in drinking water. *J. Am. Water Works Assoc.* **1980**, *72*, 695-704.
- (43) Schock, M. R. Understanding corrosion control strategies for lead. *J. Am. Water Works Assoc.* **1989**, *81*, 88-100.
- (44) Schock, M. R.; Gardels, M. C. Plumbosolvency reduction by high pH and low carbonate-solubility relationships. *J. Am. Water Works Assoc.* **1983**, *75*, 87-91.

**Table Caption**

**Table I:** Comparison of the kinetic parameters determined by the Koutecky-Levich and low overpotential methods for the electrochemical reduction of  $\text{NH}_2\text{Cl}$  and  $\text{OCl}^-$ .

**Figure Captions**

**Figure 1:** Measured equilibrium potentials (shown as open circles) for the  $\text{NH}_2\text{Cl}/\text{Cl}^-$  couple as a function of pH. A linear fit to the measured equilibrium potentials gives two linear regions. Below pH 9.4 the slope is 75 mV/pH, and above pH 9.4 the slope is 41 mV/pH. Calculated formal potentials from the Nernst equation are also shown as solid lines, which change slope at a pH of 9.25, corresponding to the  $\text{pK}_a$  of  $\text{NH}_4^+$ .

**Figure 2:** Cyclic voltammograms for the reduction (a)  $\text{OCl}^-$  and (b)  $\text{NH}_2\text{Cl}$  on a stationary Au electrode at a scan rate of 50 mV/s. The CVs were run in unstirred solutions of  $\text{OCl}^-$  and  $\text{NH}_2\text{Cl}$  of various concentrations. The pH 9 solutions were Ar purged, and contained 0.1 M  $\text{Na}_2\text{SO}_4$  and 60 mM  $\text{NaHCO}_3$ .

**Figure 3:** Linear sweep voltammograms of 1.7 mM (a)  $\text{OCl}^-$  (b)  $\text{NH}_2\text{Cl}$  on a Au rotating disk electrode at rotation rates from 700 to 2100 rpm. The voltammograms were run at a sweep rate of 50 mV/s in Ar-purged solutions containing 0.1 M  $\text{Na}_2\text{SO}_4$ , 60 mM  $\text{NaHCO}_3$  at pH 9.

**Figure 4:** Koutecky–Levich plots for 1.7 mM (a)  $\text{OCl}^-$  (b)  $\text{NH}_2\text{Cl}$  at a series of different overpotentials ( $\eta$ ). Open circuit values of 0.67 V for  $\text{OCl}^-$  and 0.47 V for  $\text{NH}_2\text{Cl}$  were used to approximate the overpotentials for determining the kinetic currents ( $i_k$ ).

**Figure 5:** Plots of  $\ln k_f(E)$  versus overpotential ( $\eta$ ) for the data obtained from the Koutecky–Levich plots shown in Figure 4. The intercept of the linear fits is  $\ln(k^\circ)$ , and the slope is proportional to the transfer coefficient ( $\alpha$ ).

**Figure 6:** Plots of current density ( $j$ ) versus overpotential ( $\eta$ ) in the small overpotential range (0 to 60 mV) for  $\text{OCl}^-$  and  $\text{NH}_2\text{Cl}$  at a rotation rate of 900 rpm in an Ar-purged solution containing 0.1 M  $\text{Na}_2\text{SO}_4$ , 60 mM  $\text{NaHCO}_3$  at pH 9. The scan rate was 1 mV/s.

**Figure 7:** Pourbaix diagram for Pb- $\text{H}_2\text{O}$ - $\text{CO}_2$  system with the concentration of dissolved Pb species equal to  $7.25 \times 10^{-8}$  M (15 ppb) and the concentration of dissolved inorganic carbon equal to  $1.5 \times 10^{-3}$  M (18 ppm) at 25 °C. Measured equilibrium potentials are shown as open squares for free chlorine, and as open circles for  $\text{NH}_2\text{Cl}$ . A linear fit to the measured equilibrium potentials for free chlorine gives two linear regions. Below pH 7.5 (corresponding to the  $\text{pK}_a = 7.5$  of  $\text{HOCl}$ ) the slope is 70 mV/pH, and above pH 7.5 the slope is 90 mV/pH.



Table 1

Species	Method				
	Koutecky–Levich plot			Low overpotential plot	
	$j_0$ (A/cm <sup>2</sup> )	$k^0$ (cm/s)	$\alpha$	$j_0$ (A/cm <sup>2</sup> )	$k^0$ (cm/s)
NH <sub>2</sub> Cl	$4.1 \times 10^{-5}$	$1.2 \times 10^{-4}$	0.2	$3.7 \pm 0.4 \times 10^{-5}$	$1.1 \pm 0.1 \times 10^{-4}$
OCl <sup>-</sup>	$8.2 \times 10^{-5}$	$2.5 \times 10^{-4}$	0.3	$7.5 \pm 0.3 \times 10^{-5}$	$2.3 \pm 0.1 \times 10^{-4}$

Figure 1

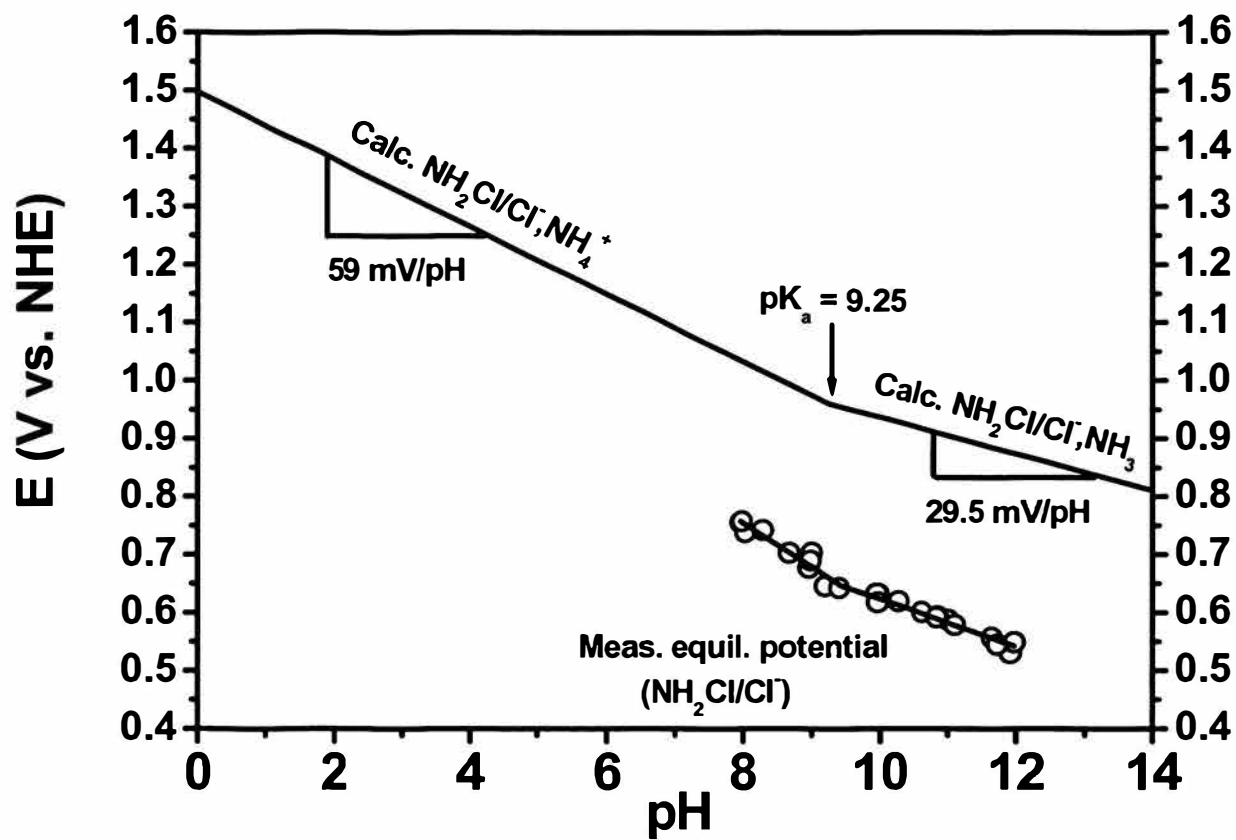


Figure 2

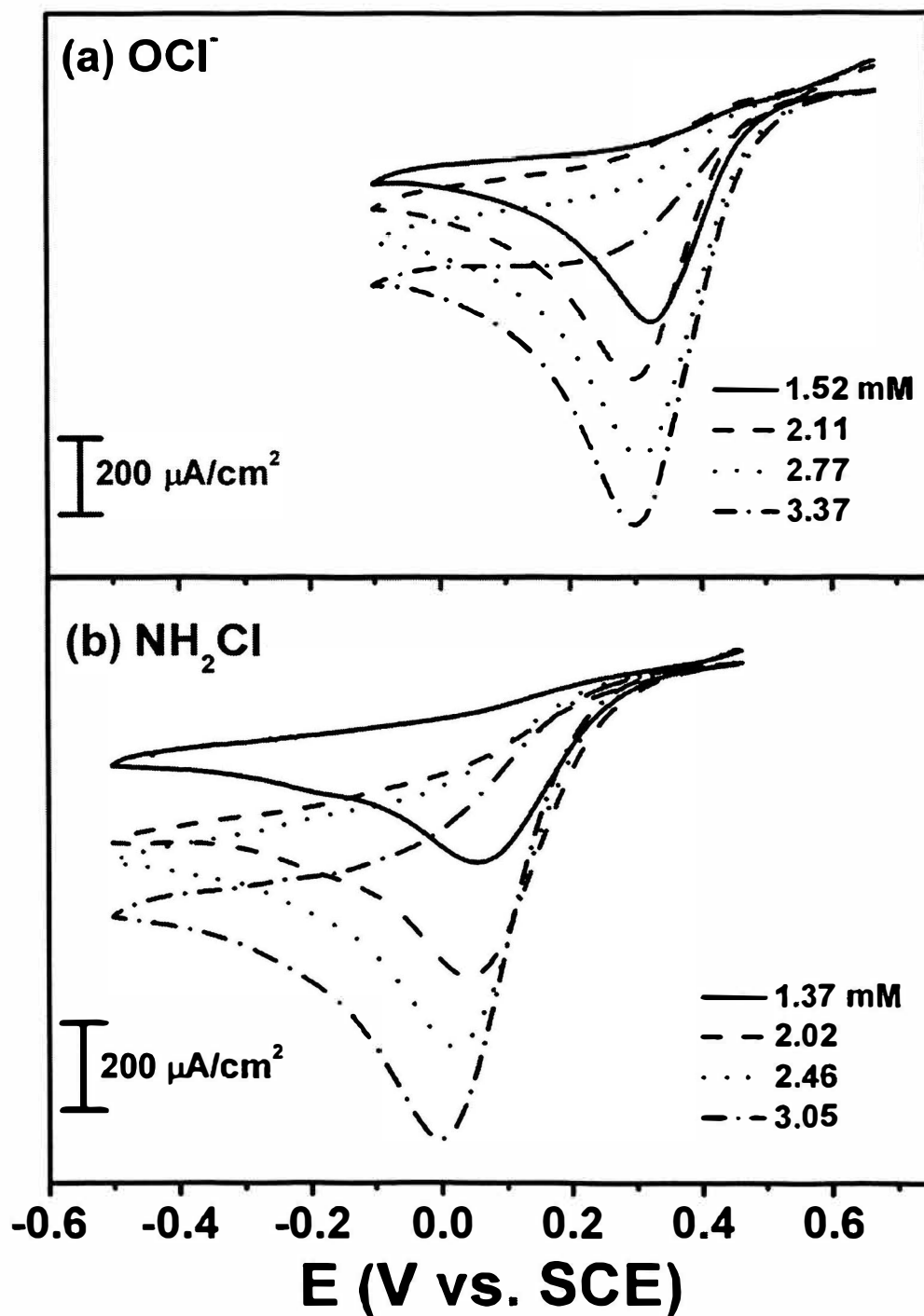


Figure 3

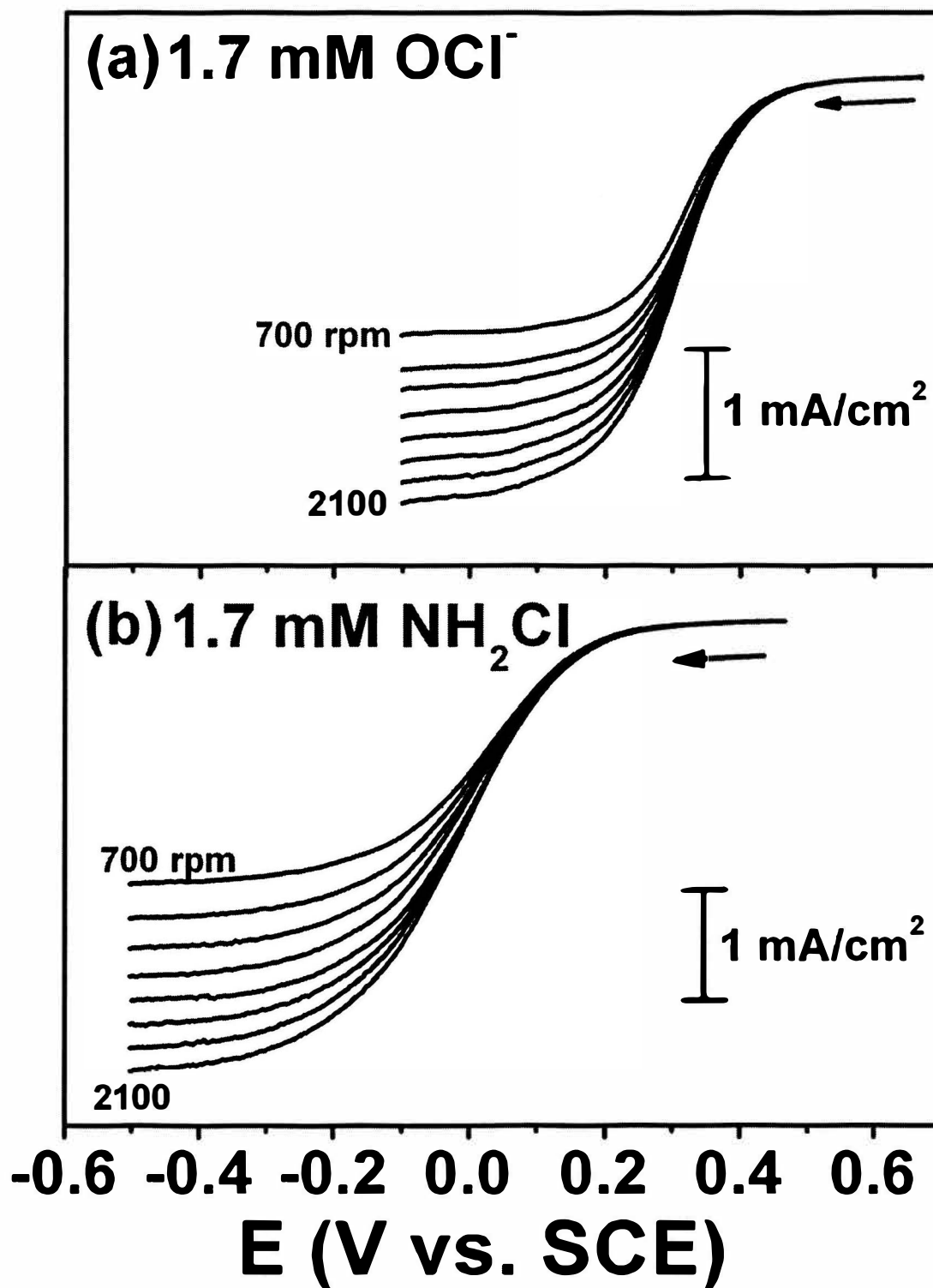


Figure 4

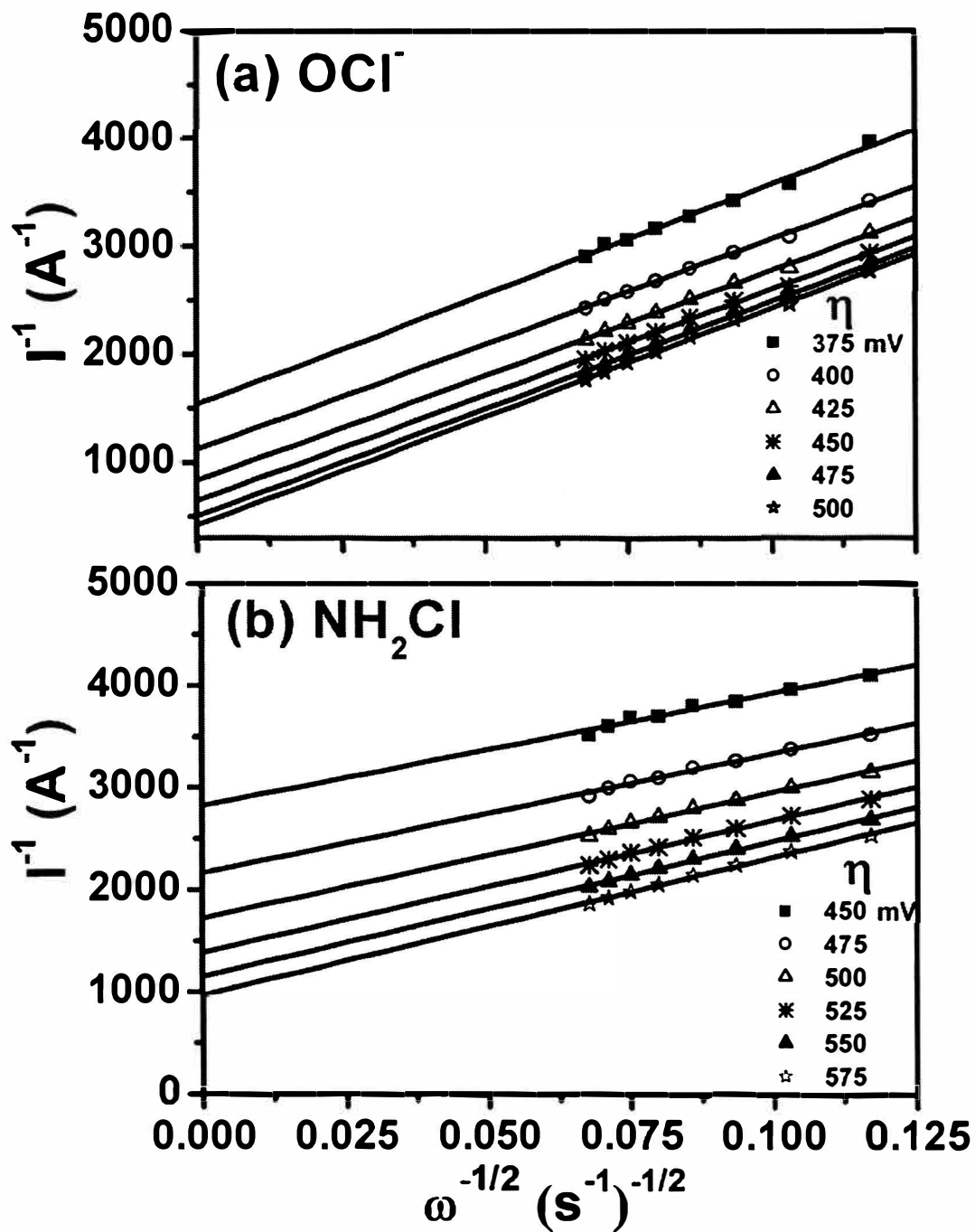


Figure 5

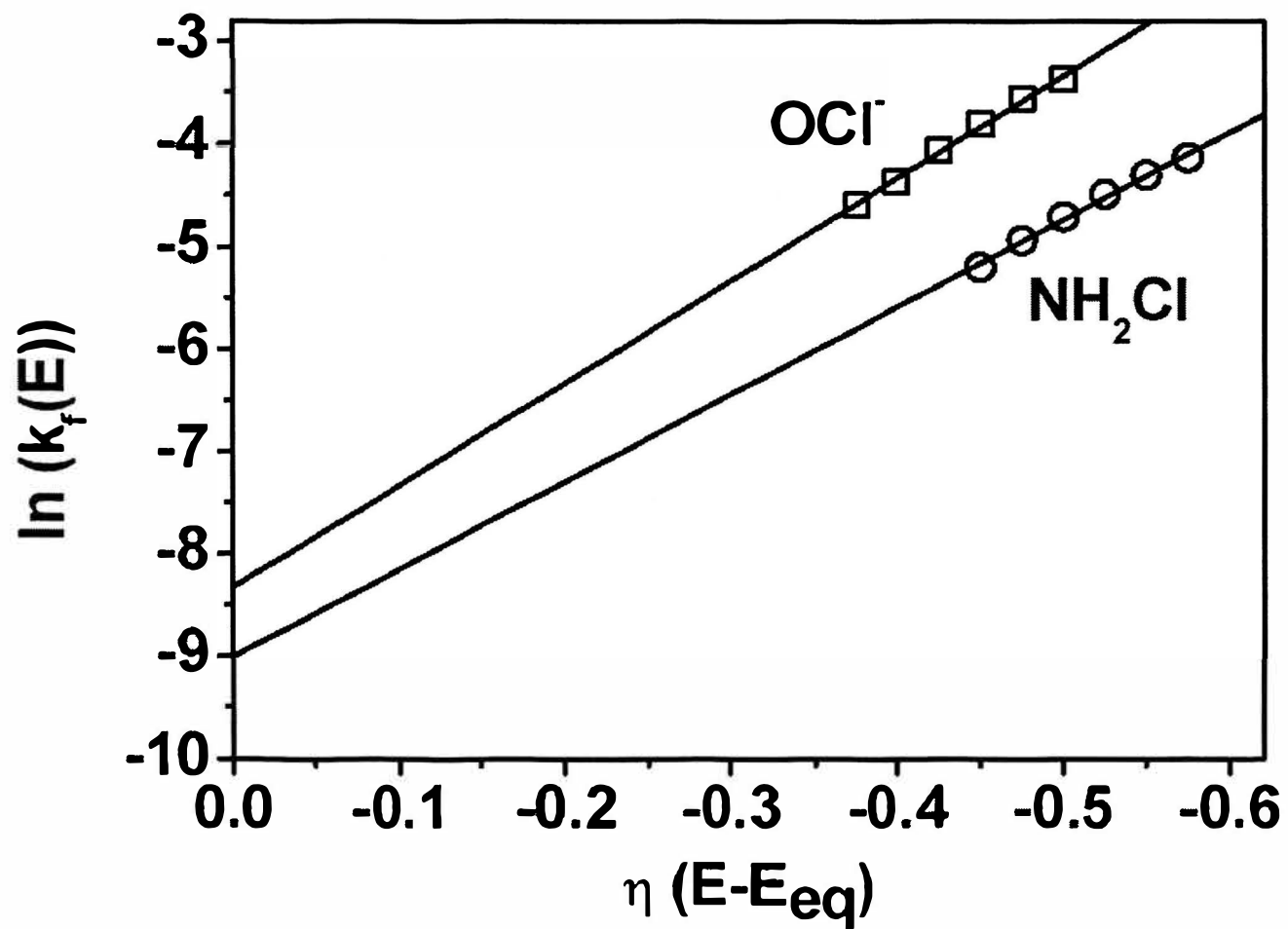


Figure 6

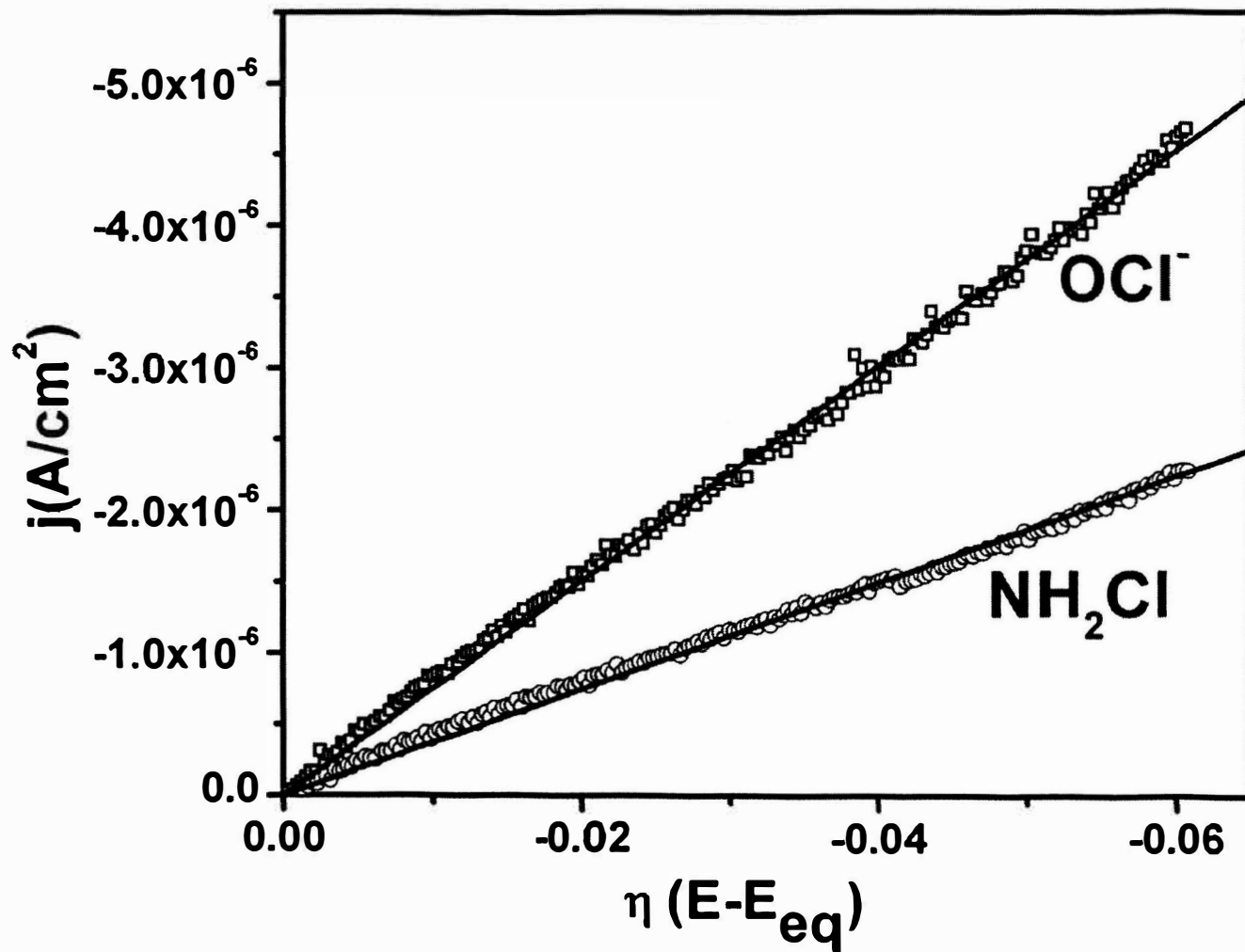


Figure 7

